Numerical simulation of domain walls in Fe whiskers and their interaction with deposited thin films

V. Christoph
HTW-Dresden, Friedrich-List-Pl. 1, D-01069 Dresden, Germany

R. Schäfer*
Leibniz Institute for Materials and Solid State Research IFW Dresden, Institute for Metallic Materials, Helmholtz-Strasse 20, D-01069 Dresden, Germany

(Received 22 June 2004; published 20 December 2004)

The domain wall structures in a single-crystalline (Fe-whisker/nonmagnetic-layer/Fe-film)–sandwich system were studied by numerical micromagnetic simulations applying a modified boundary element method. Residual stray fields, emerging from the 180° vortex wall in the whisker, are responsible for the formation of a 180° Néel wall and a head-on domain configuration in the film. Both walls are modified by mutual interaction. The calculations confirm previous experimental observations of complex magnetization processes in a 20-monolayer-thick iron film that were explained to be caused by stray-field interaction between whisker and film walls across an MgO tunneling barrier layer.

DOI: 10.1103/PhysRevB.70.214419 PACS number(s): 75.60.Ch, 75.40.Mg, 75.70.Kw, 75.70.Cn

I. INTRODUCTION

Thin film systems, in which hard and soft ferromagnetic layers are interspaced by a nonmagnetic layer, are the basis of modern magnetoelectronic devices applying the giant or tunneling magnetoresistance effects.[1] If the hard reference layer is not exchange-biased by an antiferromagnetic film, it can be demagnetized in magnetic fields much smaller than its coercive field, when these fields are used to repeatedly switch the magnetization of the adjacent soft magnetic layer.[2,3] This demagnetization, which leads to an undesired decay of the remanent moment of the hard layer, is caused by the fringing fields of Néel walls in the soft layer that easily exceed several hundred kA/m. A similar domain wall fringing field coupling effect was recently found by Kerr microscopy in a whisker-based sandwich system[4] consisting of a monocrystalline iron thin film that is deposited in close distance to the surface of an iron whisker, separated by a nonmagnetic MgO spacer layer. Residual stray fields of the whisker domain walls were identified to be responsible for complex magnetization processes in the iron film. In this article numerical micromagnetic simulations are performed to prove the existence of this stray field interaction and to understand the modification of the whisker wall structure by the presence of the iron film.

II. RECAP OF EXPERIMENTAL RESULTS

The most relevant experimental findings from Ref. 4 are summarized in Fig. 1. The magnetic ground state of an iron whisker, which is a single crystal with (100) side surfaces and a cross section of some 100×100 μm^2, consists of two domains connected by a 180° vortex domain wall that runs along the whisker axis [Fig. 1(a)]. As schematically shown in a cross-sectional view in Fig. 1(b), the vortex wall appears like a common Néel wall with (almost)in-plane rotation right at both surfaces, whereas in the volume the magnetization rotates parallel to the wall plane like in a classical Bloch wall.[5] By forming vortices close to the surfaces, stray fields are largely reduced, though not completely avoided. The residual wall fringing field was found[4] to act on an epitaxially grown iron film of 20 monolayers (ML) thickness that was interspaced by a 20-monolayer-thick MgO film. In the experiment of Fig. 1(c) both whisker and film were first saturated in the negative y direction. In a magnetic field in positive y direction a 180° wall, entering the image from the left, remagnetizes the whisker. The area of the film, which has been passed by the whisker wall, remains magnetized transversely to the whisker magnetization, either in the positive or negative x direction. Also in front of the moving whisker wall a narrow zone of transverse magnetization with an extension of some micrometers is pushed in the film, magnetized opposite to the passed zone. By depth-selective Kerr microscopy it was confirmed[4] that the sign of the transverse film domains does not depend on the surface rotation of the whisker wall, but on its internal rotation sense, which changes sign across a so-called Bloch line. The diagram in Fig. 1(d) schematically illustrates this process of stray-field writing. Here cross sections, viewed along the whisker axis, are shown. Only the Bloch part of the wall is considered, because it is responsible for the surface fringing field. This component may point in- or outwards as given by the internal rotation sense of the Bloch part. Depending on the sign of the Bloch component, either black or white transverse film domains are left behind the wall, whereas domains of opposite magnetization are pushed ahead according to the direction of the stray field. Note that the transverse film domains are again magnetized along easy crystal directions. The interaction between the whisker wall and film may also be interpreted in terms of magnetic charges [given by $\nabla\mathbf{M}(\mathbf{r})$, where $\mathbf{M}(\mathbf{r})$ is the magnetization distribution in units of (A/m)] as sketched in Fig. 1(e). The charge of the whisker wall at the surface is matched by opposite charges in the film. These are created by the formation of a head-on 180

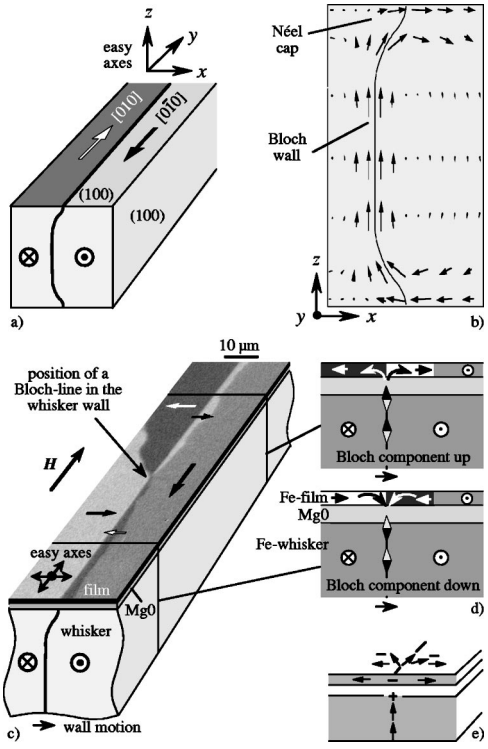

FIG. 1. (a) Basic domain geometry in an iron whisker, together with the coordinate system used for the calculations. (b) Cross-sectional view of the vortex wall separating the 180° domains (schematically, after Ref. 6). Shown is the projection of the magnetization vector onto the cross section. The contour line indicates the center of the wall, i.e., the surface on which the *y* component passes through zero. (c) Kerr image of the domains in the Fe film (graphically distorted to create a perspective view) of the Fe-whisker/MgO (20 ML)/Fe-film (20 ML) system, after a 180° whisker wall has entered from the left. (d) Switching of the Fe film, induced by the fringing field of the moving whisker wall. Only the Bloch component of the whisker wall is considered in these cross-sectional schematics. (e) Magnetic charges (after Ref. 4).

Néel wall in the film, which is supported by the crystal anisotropy that provides the transverse easy directions.

III. MICROMAGNETIC SIMULATIONS

The existence of magnetic surface charges for vortex walls in iron was already proven by numerical micromagnetic calculations (e.g., Refs. 7 and 8). Although they were performed for iron films in the micrometer thickness range rather than for bulk crystals like whiskers, a small magnetization component perpendicular to the surface was found when the wall meets the surface, despite the overall vortex wall structure. Also, scanning electron microscopy with polarization analysis (SEMPA) observations of walls on iron sheets were explained in terms of a small out-of-plane component.[9–11]

To simulate the interaction between the whisker and film we performed micromagnetic simulations using a modified boundary element method.[12] This method is especially well adapted for the calculation of stray fields for all systems where the magnetic bodies can be subdivided into elements whose magnetization can be approximated by a constant vector. The theoretical approach to self-consistent magnetization and field distributions described below is very similar to the processes taking place in the magnetic system itself. Once the magnetization distribution has been calculated, the magnetic charges at the boundaries of the elements are known and the calculation of the stray field becomes trivial everywhere. The magnetization distribution $\mathbf{M}(\mathbf{r})$ is calculated by assuming the direction of the magnetization in the whisker and layer to be parallel to a local effective field,

$$\mathbf{M} = M_s \frac{\mathbf{H}(\mathbf{r})}{|\mathbf{H}(\mathbf{r})|}, \tag{1}$$

where M_s is the saturation magnetization and $\mathbf{H}(\mathbf{r})$ denotes the local effective field. The latter is the sum of external field $\mathbf{H}_0$, magnetostatic interaction (stray) field $\mathbf{H}_s(\mathbf{r})$, exchange (molecular) field $\mathbf{H}_{ex}$, and anisotropy field $\mathbf{H}_{an}$. Subdividing whisker and layer into small volume elements (cuboids) located at positions r_i with boundary surface elements S_{ij} (rectangles, $j=1, 6$) the stray field can be calculated by

$$\mathbf{H}_s(\mathbf{r}) = \sum_i \sum_j \int_{S_{ij}} dS[\mathbf{M}(\mathbf{r}) \cdot \mathbf{n}_{ij}] \frac{\mathbf{r}-\mathbf{r}_i}{|\mathbf{r}-\mathbf{r}_i|^3}, \tag{2}$$

where $\mathbf{n}_{ij}$ denotes the normal unit vector of the surface element S_{ij}. The surface integrals in Eq. (2) can be calculated exactly, and for volume elements sufficiently small Eq. (2) is a good approximation for the stray field. The exchange field is given by

$$\mu_0 \mathbf{H}_{ex} = \frac{A}{M_s^2} \nabla^2 \mathbf{M}(\mathbf{r}), \tag{3}$$

where $A = 10^{-11}$ J/m is the exchange constant used for iron in our calculations. For cubic ferromagnets the anisotropy field follows from the anisotropy energy $W_{an} = K_1(M_x^2 M_y^2 + M_x^2 M_z^2 + M_y^2 M_z^2)/M_s^4$. Using $\mu_0 H_{an} = \partial W_{an}/\partial \mathbf{M}_{an}$ and taking into account $M_x^2 + M_y^2 + M_z^2 = M_s^2$, it follows that

$$\mu_0 H_{an,i} = K_1 M_i (3M_i^2 - M_s^2)/M_s^4, \quad i = x,y,z. \tag{4}$$

Equations (2)–(4) have been solved by an iteration procedure starting from a magnetization distribution where the left and right hand sides of the whisker and film are saturated in opposite directions, i.e., $M_y = \pm M_s$ and $M_x = M_z = 0$ everywhere. To restrict the number of elements, the magnetization was assumed to be independent of the *y* coordinate, i.e., the *y* dimension of the elements goes to infinity. Because of this approximation the calculation is restricted to a region far from the Bloch line shown in Fig. 1(c). Furthermore the *x* and *z* dimensions of the elements were chosen to be dependent on the variability of the magnetization distribution. For the numerical calculation, a total of 2900 volume elements in the whisker and 600 elements in the film was adopted. The smallest elements had a width of 20 nm in the *x* direction and 1.5 nm in *z* direction. The dimensions of the elements have been augmented gradually up to 500 nm in the film (*x* direction) at a distance of 1.5 μm from the wall center and up to 200 nm into the depth of the whisker (*z* direction). The

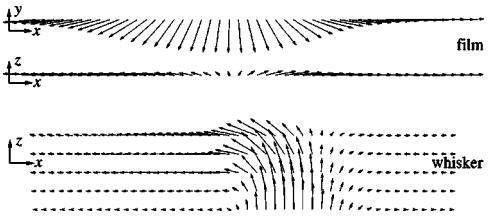

FIG. 2. Magnetization vector plot in the vicinity of the domain walls in whisker and film (the image width is 120 nm). Plotted is the projection of the magnetization vector on the drawing plane for the coordinates as indicated. The whisker magnetization is shown down to a depth of 20 nm from the surface, i.e., the distance between the plotted layers is 5 nm. Two projections are shown for the iron film.

whisker was segmented down to a depth of 2 μm below its surface; for larger depths the magnetization distribution was assumed independent of the z coordinate (depth). The iron film with a thickness of 3 nm was separated by a nonmagnetic spacer layer of 4 nm from the whisker surface. These values approximately correspond to the 20-monolayer thicknesses of iron and MgO films used in the experiment[4] (note that the monolayer distance is half the lattice constant in each case, the latter being 0.4212 and 0.2866 nm for MgO and iron, respectively). Using the constants $K_1=4.8\times10^4$ J/m^3 and $\mu_0 M_s=2.1$ T, both in the whisker and the Fe film a self-consistent solution for the magnetization distribution has been obtained.[13] Note that the magnetostrictive self-energy was not considered in our calculations.

IV. RESULTS AND DISCUSSION

The magnetization distributions in the whisker and film in the neighborhood of the 180° whisker domain wall are illustrated in Fig. 2. Plotted are the magnetization components m_x, m_z for some representative layers in the whisker and the components m_x, m_z as well as m_x, m_y in the iron film (with $\mathbf{m}=\mathbf{M}/M_s$). As expected, a 180° head-on wall of Néel character is in fact formed in the film, laterally somewhat displaced from the center of the whisker wall. Also evident is the vortex character of the whisker wall with a considerable z component at the whisker surface and an asymmetric overall profile.

As shown explicitly in Fig. 3, deep inside the whisker (200 nm below the surface in the figure) the domain wall is a simple symmetric Bloch-type wall, i.e., the magnetization rotates parallel to the wall plane in a stray-field-free manner. A width of 36 nm is derived for the Bloch part of the wall by evaluating the slope of the magnetization angle according to Lilley (see p. 219 in Ref. 5). The center of this Bloch wall determines the origin of the x axis for all the following plots. Near the whisker surface the wall profile becomes asymmetric with a strong in-plane component. This is evident in Fig. 4, where the magnetization components in the whisker 2.5 nm below its surface are plotted in the absence (bold curves) and presence (thin curves) of the iron film.

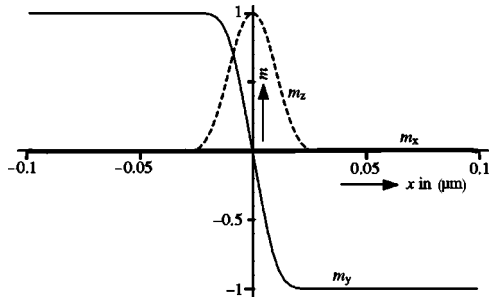

FIG. 3. Bulk domain wall profiles in the whisker at a depth of 200 nm. The structure was calculated in the absence of the iron film.

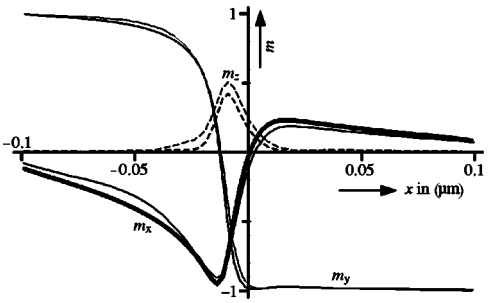

FIG. 4. Wall profiles in the whisker at a depth of 2.5 nm below the surface, calculated in the presence (thin curves) and absence (bold curves) of the iron film.

The considerable z component at the whisker surface induces a head-on wall in the iron film, the profiles of which are plotted in Fig. 5. This wall is of Néel type (i.e., the magnetization primarily rotates parallel to the film plane) with a small out-of-plane magnetization component m_z, caused by the stray field of the Bloch-type wall in the whisker. The change of the whisker wall magnetization in the presence of the iron film was already demonstrated in Fig. 4. The out-of-plane component m_z in the whisker is considerably influenced by the magnetic film while the other components remain largely unchanged. The magnetization profiles in the whisker volume (see Fig. 3) are not altered by the presence of the iron film.

In Fig. 6 the magnetic field components H_x and H_z in the gap between whisker and iron film are plotted as a function of the coordinate x perpendicular to the wall. The magnetic field points away from the wall on both sides and has a positive z component near the wall and a negative z component at larger distance (see inset in Fig. 6). Thereby the mag-

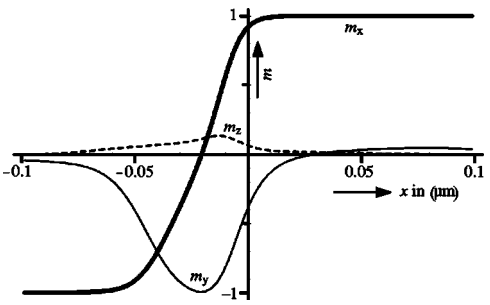

FIG. 5. Magnetization distribution of the 180° head-on domain wall in the deposited iron film.

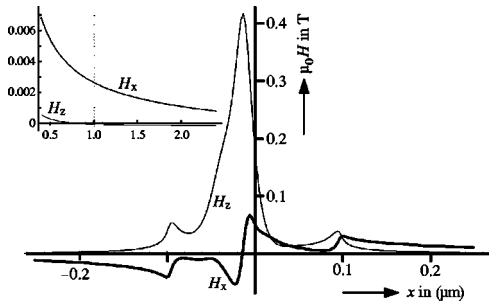

FIG. 6. In- and out-of-plane components of the magnetic field for the whisker-film system, calculated 2 nm above the whisker surface in the nonmagnetic gap between whisker and film. The inset shows an enlarged view at larger distance, revealing a change of sign in the H_z component.

netic flux, originated in the whisker wall, is directed back to the whisker. Different from the situation in the whisker, in the iron film the magnetization far from the wall cannot be stabilized in the direction parallel to the wall (y direction), i.e., in an iteration process the transverse film domains ($M_x = -M_s$ and $M_x = M_s$) on both sides of the Néel-type wall increase infinitely. A finite-sized transverse domain of some micrometer extension, as experimentally observed in the film [see the transverse zone in front of the moving wall in Fig. 1(c)], would require stabilization in our calculations by the introduction of pinning centers.

Note that the calculated domain wall widths of about 30 to 50 nm are much smaller than those experimentally observed.[4] The reason is that in the modeled whisker (where a cubic crystal anisotropy and a infinite extension in y direction were taken into consideration) the Bloch wall width is not well defined. The magnetization vector in this wall rotates parallel to the (100) plane. In the wall center it therefore meets the $+y$ or $-y$ easy crystal direction. Thus the anisotropy energy in the center is the same as in the adjacent domains. It is therefore expected that the (100) 180° wall tends to split into two separate (100) 90° walls by inserting a domain that is magnetized along the plus or minus y direction. Such a domain, however, is elastically incompatible with the outer domains for magnetostrictive reasons. The magnetostrictive self-energy therefore leads to a contraction of the wall and prevents the divergence of the wall width as reviewed in Chap. 3.6.1 of Ref. 5. To prevent a divergence of the Bloch wall in the x direction in our calculations, a small but finite external magnetic field along the z axis was added. Then a wall width of 36 nm for the Bloch wall in the volume of the whisker was obtained that is close to $\pi\sqrt{A/K_1} = 45$ nm. Taking into acccount the magnetostrictive self-energy a Bloch wall width of more than $10\sqrt{A/K_1}$ was theoretically predicted (see page 233 in Ref. 5). Also, the finite whisker width serves in preventing the wall divergence (a complicated closure domain structure at the whisker surfaces would be required in case of a decaying 180° wall, i.e., a 90° domain arrangement). Consequently, by introducing a small field in the z direction for mapping the influence of the magnetostriction and the finite whisker width, it is likely that the calculated wall in the whisker and consequently the film wall will be narrower than in reality. The fundamental predictions about the interaction mechanism between whisker and film, however, will still be valid despite this simplification.

V. SUMMARY

By numerical micromagnetic simulations it was proven that an asymmetric vortex wall in an iron whisker creates a 180°-head-on Néel wall in an iron film that is deposited in close distance to the surface of the whisker. Residual stray fields of the whisker wall are responsible for this interaction effect. In addition, close to whisker surface the whisker wall structure is modified by the presence of the film.

ACKNOWLEDGMENT

The critical reading of the manuscript by Jeffrey McCord is gratefully acknowledged.

*Electronic address: r.schaefer@ifw-dresden.de

[1] *Magnetic Multilayers and Giant Magnetoresistance*, edited by U. Hartmann (Springer Verlag, Berlin, 2000).
[2] L. Thomas, M. Samant, and S. S. P. Parkin, Phys. Rev. Lett. **84**, 1816 (2000).
[3] L. Thomas, J. Lüning, A. Scholl, F. Nolting, S. Anders, J. Stöhr, and S. S. P. Parkin, Phys. Rev. Lett. **84**, 3462 (2000).
[4] R. Schäfer, R. Urban, D. Ullmann, H. L. Meyerheim, B. Heinrich, L. Schultz, and J. Kirschner, Phys. Rev. B **65**, 144405 (2002).
[5] A. Hubert and R. Schäfer, *Magnetic Domains: The Analysis of Magnetic Microstructures* (Springer Verlag, Berlin, 1998).
[6] A. Hubert, Z. Angew. Phys. **32**, 58 (1971).
[7] M. R. Scheinfein, J. Unguris, J. L. Blue, K. J. Coakley, D. T. Pierce, R. J. Celotta, and P. J. Ryan, Phys. Rev. B **43**, 3395 (1991).
[8] A. Aharoni and J. P. Jakubovics, Phys. Rev. B **43**, 1290 (1991).
[9] H. P. Oepen and J. Kirschner, Phys. Rev. Lett. **62**, 819 (1989).
[10] M. R. Scheinfein, J. Unguris, R. J. Celotta, and D. T. Pierce, Phys. Rev. Lett. **63**, 668 (1989).
[11] O. S. Anilturk and A. R. Koymen, J. Magn. Magn. Mater. **213**, 281 (2000).
[12] V. Christoph, S. Wirth, and S. von Molnar, J. Appl. Phys. **89**, 7472 (2001).
[13] The iteration was continued as long as any magnetic charge in the system varied more than 0.1%. To avoid a "pulsation" of the magnetization distribution a relaxation method was used. For a total number of 1500 iterations, a CPU time of about 15 h on a conventional PC was needed.